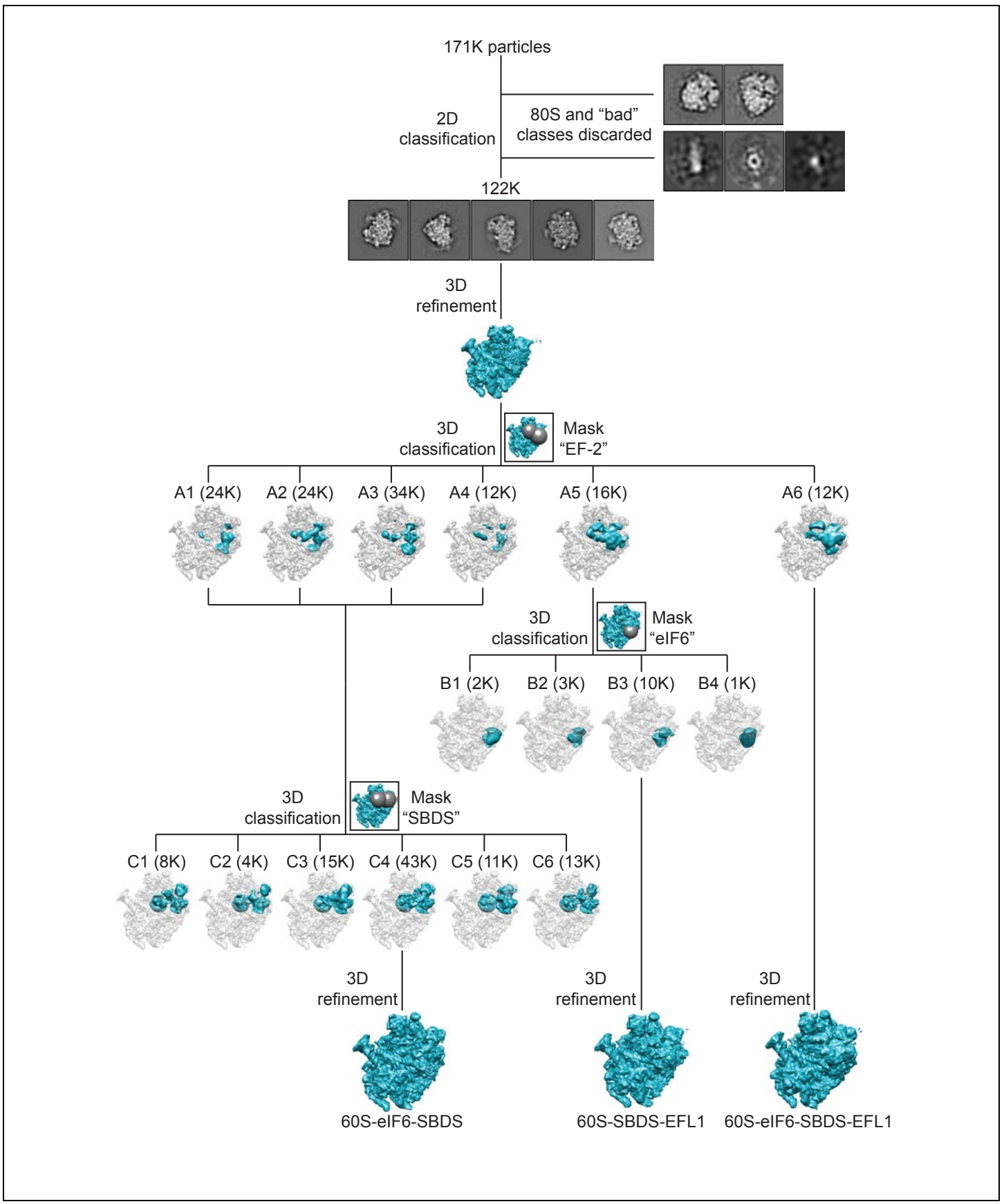
171K particles
2D classification
80S and "bad" classes discarded
122K
3D refinement
3D classification
Mask "EF-2"
A1 (24K)
A2 (24K)
A3 (34K)
A4 (12K)
A5 (16K)
A6 (12K)
3D classification
Mask "eIF6"
B1 (2K)
B2 (3K)
B3 (10K)
B4 (1K)
3D classification
Mask "SBDS"
C1 (8K)
C2 (4K)
C3 (15K)
C4 (43K)
C5 (11K)
C6 (13K)
3D refinement
3D refinement
3D refinement
60S-eIF6-SBDS
60S-SBDS-EFL1
60S-eIF6-SBDS-EFL1

Supplementary Figure 1

Overview of cryo-EM image processing procedure.

Maximum likelihood classification scheme and masks used to obtain the complexes of eIF6, SBDS and EFL1 bound to the 60S ribosomal subunit. Insets show the position of the spherical masks (grey) on the 60S subunit (cyan).

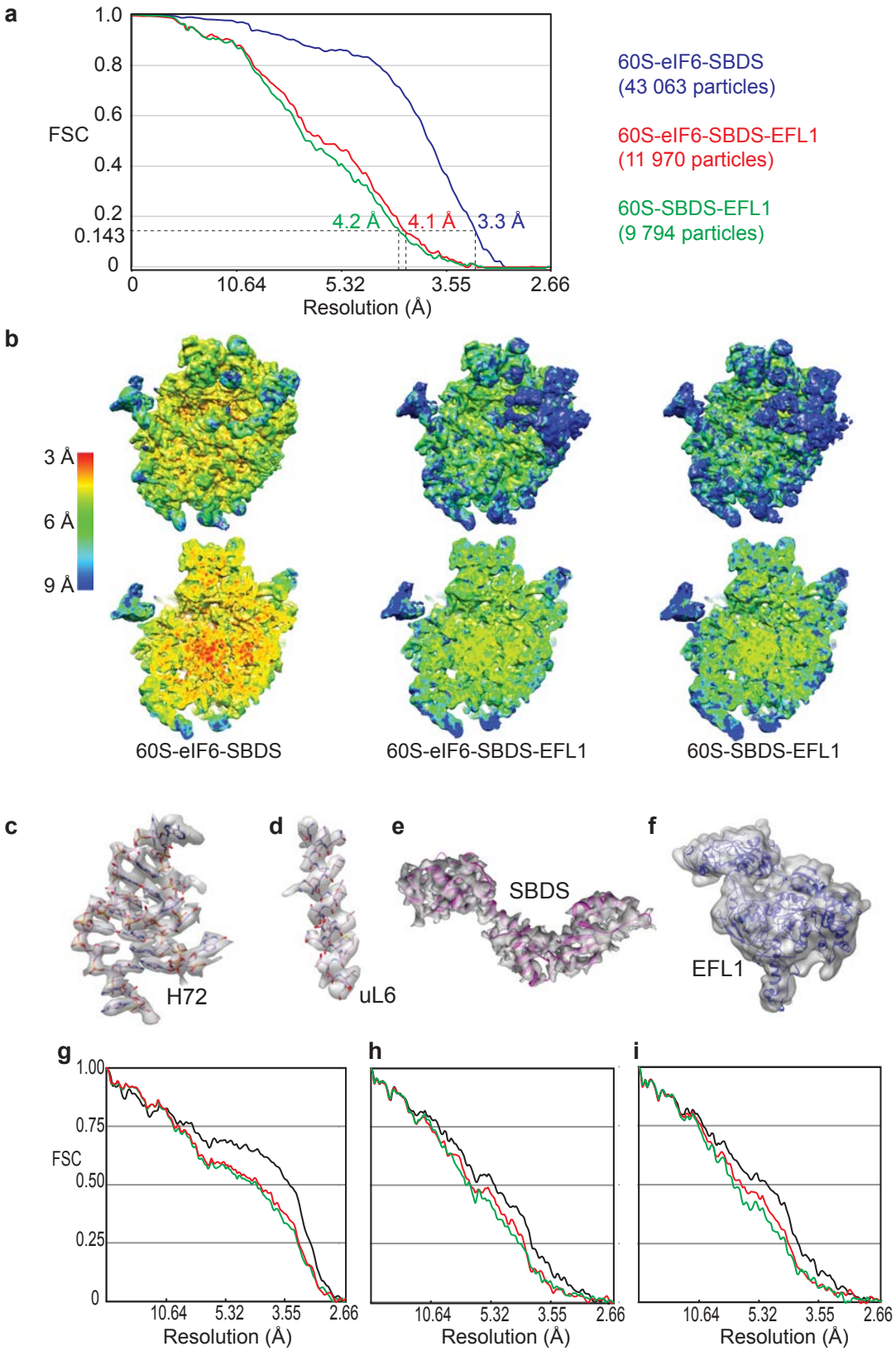
a
1.0
0.8
0.6
FSC
0.4
0.2
0.143
0
4.2 Å
4.1 Å
3.3 Å
0
10.64
5.32
3.55
2.66
Resolution (Å)
60S-eIF6-SBDS
(43 063 particles)
60S-eIF6-SBDS-EFL1
(11 970 particles)
60S-SBDS-EFL1
(9 794 particles)
b
3 Å
6 Å
9 Å
60S-eIF6-SBDS
60S-eIF6-SBDS-EFL1
60S-SBDS-EFL1
c
H72
d
uL6
e
SBDS
f
EFL1
g
h
i
1.00
0.75
FSC
0.50
0.25
0
10.64
5.32
3.55
2.66
Resolution (Å)

Supplementary Figure 2

Resolution of the 60S ribosomal subunit complexes and validation of the atomic model.

(a) Gold-standard Fourier shell correlation (FSC) curves for the three 60S ribosome complexes after 3D refinement and statistical movie processing in RELION (Bai, X. C. *et al*., *Elife* **2**, e00461, 2013; Scheres, S. H. *J Struct Biol* **180**, 519-530, 2012).

(b) Surface (top panel) and cross-sectional (bottom panel) views of the unsharpened final maps colored according to local resolution calculated with the ResMap software package (Kucukelbir, A. *et al.*, *Nat Methods,* **11**, 63-65, 2014).

(c, d, e, f) Examples of densities with the model fitted showing helix 72 of the 26S rRNA from the 60S-eIF6-SBDS complex with the density filtered at 3.3 Å (**c)**, α-helix of the uL6 protein from the 60S-eIF6-SBDS complex with the density filtered at 3.3 Å (**d**), SBDS from the 60S-eIF6-SBDS complex with the density is filtered at 4 Å (**e**), EFL1 from the 60S-eIF6-SBDS-EFL1 complex with the density is filtered at 8 Å (**f**).

(g, h, i) Cross-validation against over-fitting. FSC curves are shown for the 60S-eIF6-SBDS (**g**), 60S-eIF6-SBDS-EFL1 (**h**) and 60S-SBDS-EFL1 (**i**) complexes between the final refined atomic model and the reconstructions from all particles (black); between the model refined in the reconstruction from only half of the particles and the reconstruction from that same half (FSC_{work}, red); and between that same model and the reconstruction from the other half of the particles (FSC_{test}, green).

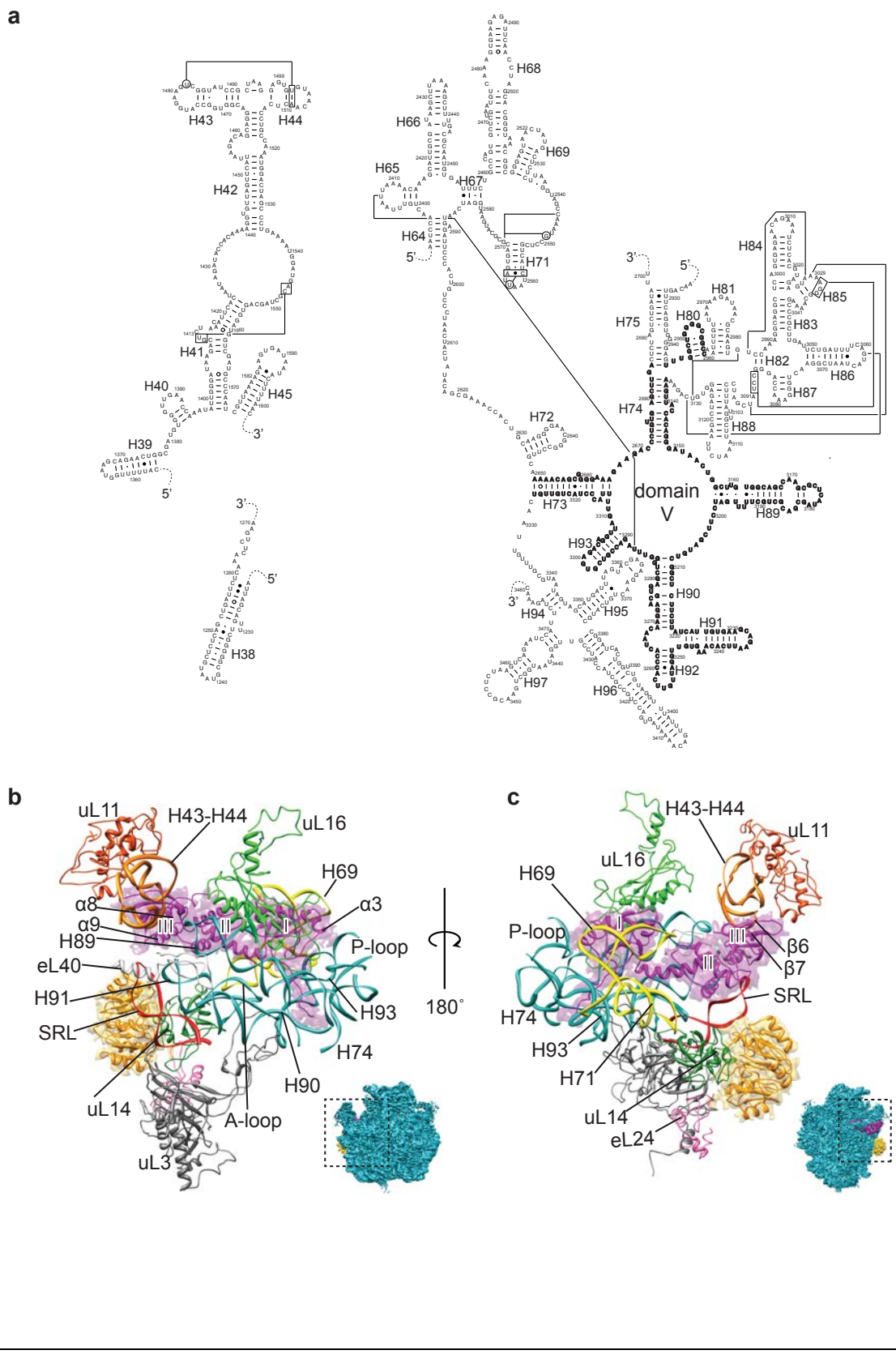
a
H43
H44
H42
H41
H40
H45
H39
3'
5'
H38
H68
H66
H69
H65
H67
H64
H71
H72
H73
domain
V
H84
H85
H81
H75
H80
H83
H82
H86
H87
H74
H88
H89
H93
H90
H94
H95
H91
H92
H97
H96
b
uL11
H43-H44
uL16
H69
α8
α3
α9
H89
P-loop
eL40
H91
H93
SRL
H74
H90
uL14
A-loop
uL3
180°
c
H43-H44
uL11
uL16
H69
P-loop
β6
β7
SRL
H74
H93
H71
uL14
eL24

Supplementary Figure 3

Atomic models of the 60S-SBDS-eIF6 complex.

(a) Secondary structure diagram of modeled *Dictyostelium* 26S rRNA. The diagram was modified from *S. cerevisiae* 25S rRNA (Comparative RNA Web Site, www.rna.ccbb.utexas.edu). The PTC is shown in bold. Base pairs involved in tertiary interactions are indicated with lines connecting the circles or boxes around the bases involved in the interaction. (-) corresponds to canonical base pairs, while (•, ○ and ●) correspond to non-canonical base pairs.

(b, c) Back (**b**) and front (**c**) views of the atomic model of the 60S-eIF6-SBDS complex. SRL, sarcin-ricin loop.

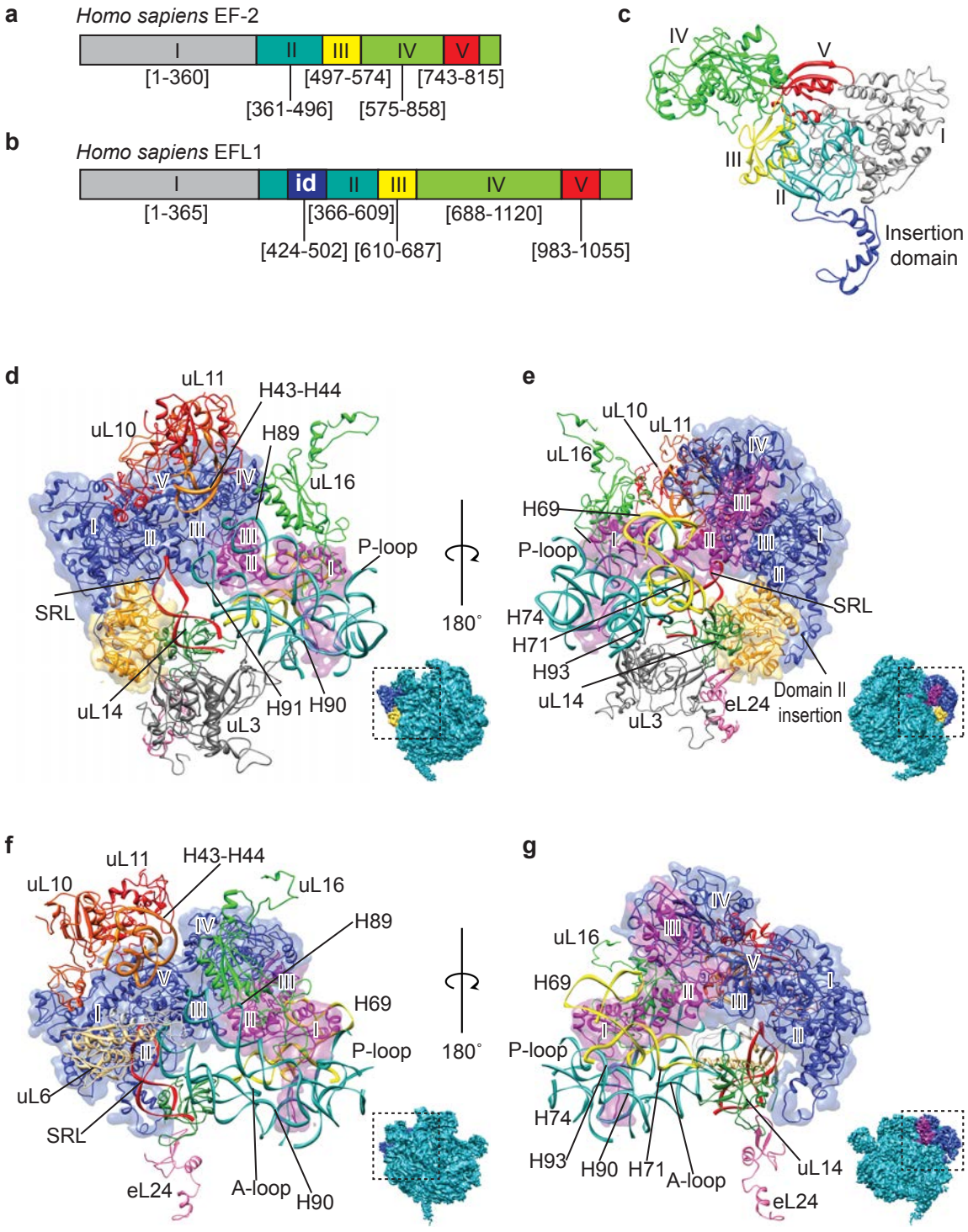
a
Homo sapiens EF-2
I
II
III
IV
V
[1-360]
[361-496]
[497-574]
[575-858]
[743-815]
b
Homo sapiens EFL1
I
id
II
III
IV
V
[1-365]
[366-609]
[424-502]
[610-687]
[688-1120]
[983-1055]
c
IV
V
I
III
II
Insertion domain
d
uL11
H43-H44
uL10
H89
uL16
P-loop
SRL
uL14
H91
H90
uL3
180˚
e
uL10
uL11
uL16
H69
P-loop
H74
H71
H93
uL14
uL3
eL24
SRL
Domain II insertion
f
uL11
H43-H44
uL10
uL16
H89
H69
P-loop
uL6
SRL
eL24
A-loop
H90
180˚
g
uL16
H69
P-loop
H74
H93
H90
H71
A-loop
uL14
eL24

Supplementary Figure 4

Molecular environment of eIF6, SBDS and EFL1.

(**a, b**) Schematic representations of *Homo sapiens* EF-2 (**a**) and EFL1 (**b**).

(c) Ribbon representation of the atomic model of human EFL1 with the subdomain structure highlighted using the same color scheme as (**b**).

(d-g) Back (**d, f**) and front (**e, g**) views of the atomic models of the 60S-eIF6-SBDS-EFL1 and 60S-SBDS-EFL1 complexes, respectively. SRL, sarcin-ricin loop.

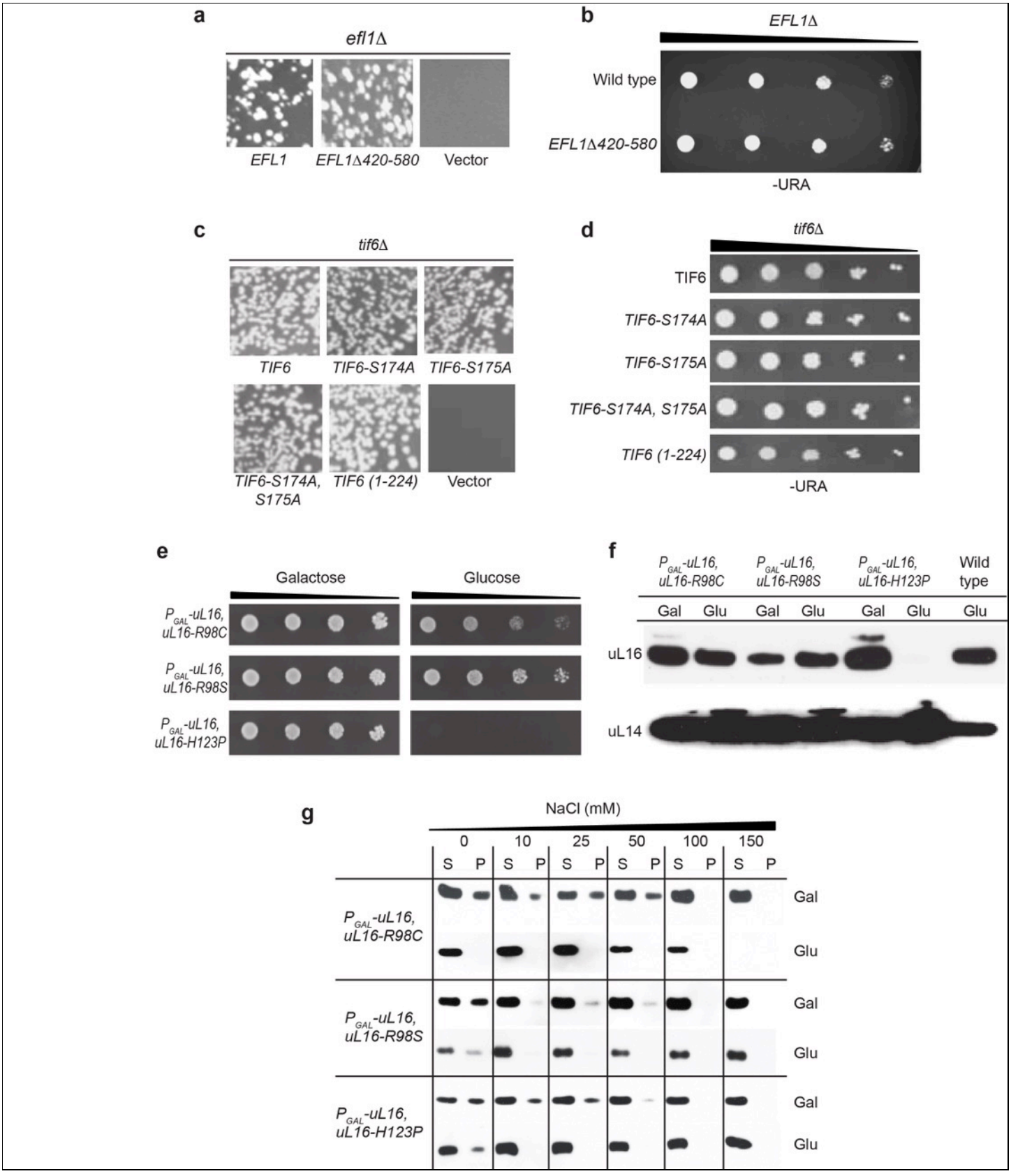
a
efl1Δ
EFL1
EFL1Δ420-580
Vector
b
EFL1Δ
Wild type
EFL1Δ420-580
-URA
c
tif6Δ
TIF6
TIF6-S174A
TIF6-S175A
TIF6-S174A, S175A
TIF6 (1-224)
Vector
d
tif6Δ
TIF6
TIF6-S174A
TIF6-S175A
TIF6-S174A, S175A
TIF6 (1-224)
-URA
e
Galactose
Glucose
PGAL-uL16, uL16-R98C
PGAL-uL16, uL16-R98S
PGAL-uL16, uL16-H123P
f
PGAL-uL16, uL16-R98C
PGAL-uL16, uL16-R98S
PGAL-uL16, uL16-H123P
Wild type
Gal Glu Gal Glu Gal Glu Glu
uL16
uL14
g
NaCl (mM)
0 10 25 50 100 150
S P S P S P S P S P S P
PGAL-uL16, uL16-R98C
PGAL-uL16, uL16-R98S
PGAL-uL16, uL16-H123P
Gal
Glu

Supplementary Figure 5

uL16 is required to recruit Sdo1 to the 60S subunit *in vivo.*

(a) The EFL1 domain II insertion is dispensable *in vivo*. Random sporulation assay showing *efl1Δ* cells transformed with empty vector (pRS316) control or plasmids expressing wild type *EFL1* or the *EFL1Δ420-580* mutant (left).

(b) Tenfold serial dilutions (left to right) of the indicated yeast cells spotted onto selective –URA medium (left). *efl1Δ* cells transformed with empty vector (pRS316) are non-viable and are therefore not shown.

(c) S174 and S175 are dispensable for Tif6 function *in vivo*. Random sporulation assay showing *tif6Δ* cells transformed with empty vector (pRS316) control or plasmids expressing wild type *TIF6* or the indicated *TIF6* mutants.

(d) Tenfold serial dilutions (left to right) of the indicated yeast strains spotted onto selective –URA medium (left). *tif6Δ* cells transformed with empty vector (pRS316) are non-viable and are therefore not shown.

(e) Severe fitness defect of the *uL16-H123P* allele. Indicated yeast cells with (galactose) or without (glucose) endogenous uL16 spotted in tenfold serial dilutions (left to right) onto solid media.

(f) The *uL16-H123P* allele markedly reduces uL16 expression. uL16 and uL14 (control) were visualized by immunoblotting of extracts from the indicated strains with (galactose) or without (glucose) endogenous uL16. As controls, uL16 and uL14 were visualized by immunoblotting of extracts from strain C375 (wild type).

(g) The T-ALL associated alleles *uL16-H123P*, *uL16-R98S* and *uL16-R98C* impair Sdo1 binding to the 60S subunit *in vivo*. Sdo1-FLAG or uL14 were visualized by immunoblotting of supernatant (S) or pellet (P) from cell extracts with (galactose) or without (glucose) endogenous uL16 across the indicated range of NaCl concentrations.